AGU PUBLICATIONS

Geophysical Research Letters

RESEARCH LETTER
10.1002/2017GL073926

Key Points:
- In the period of 2011–2015, sea level rise decelerated north of Cape Hatteras and accelerated south of the Cape to >3 times the global mean
- Comparable sea level rise accelerations (hot spots) have occurred over ~1500 km stretches of the eastern United States in the last 95 years
- The North Atlantic Oscillation determines the latitudinal position of hot spots, while ENSO is related to their timing

Supporting Information:
- Supporting Information S1

Correspondence to:
A. Valle-Levinson,
arnoldo@ufl.edu

Citation:
Valle-Levinson, A., A. Dutton, and J. B. Martin (2017), Spatial and temporal variability of sea level rise hot spots over the eastern United States, *Geophys. Res. Lett.*, *44*, 7876–7882, doi:10.1002/2017GL073926.

Received 21 APR 2017
Accepted 9 JUL 2017
Accepted article online 9 AUG 2017
Published online 12 AUG 2017

Spatial and temporal variability of sea level rise hot spots over the eastern United States

Arnoldo Valle-Levinson[1], Andrea Dutton[2], and Jonathan B. Martin[2]

[1]Department of Civil and Coastal Engineering, University of Florida, Gainesville, Florida, USA, [2]Department of Geological Sciences, University of Florida, Gainesville, Florida, USA

Abstract Regional sea level rise (SLR) acceleration during the past few decades north of Cape Hatteras has commonly been attributed to weakening Atlantic Meridional Overturning Circulation, although this causal link remains debated. In contrast to this pattern, we demonstrate that SLR decelerated north of Cape Hatteras and accelerated south of the Cape to >20 mm/yr, > 3 times the global mean values from 2011 to 2015. Tide gauge records reveal comparable short-lived, rapid SLR accelerations (hot spots) that have occurred repeatedly over ~1500 km stretches of the coastline during the past 95 years, with variable latitudinal position. Our analysis indicates that the cumulative (time-integrated) effects of the North Atlantic Oscillation determine the latitudinal position of these SLR hot spots, while a cumulative El Niño index is associated with their timing. The superposition of these two ocean-atmospheric processes accounts for 87% of the variance in the spatiotemporal pattern of intradecadal sea level oscillations.

1. Introduction

With continued sea level rise (SLR), coastal communities are increasingly threatened by storm surges as well as loss of coastal land and water resources [*Wahl et al.*, 2015; *Neumann et al.*, 2015]. Informing these communities for future SLR requires an understanding of the timescales and magnitudes of ocean dynamics that influence regional patterns of sea level change. Local or regional rates of SLR may exceed the global mean because of a suite of factors related to ocean-atmosphere interactions (e.g., wind and current strength) or static equilibrium processes, e.g., melting land ice [*Stammer et al.*, 2013]. In addition to this spatial variability, temporal variability in rates of SLR at intradecadal to multidecadal timescales occurs superimposed upon the longer-term signal of SLR. The combined spatiotemporal variability may result in regions with enhanced vulnerability caused by accelerating sea level rise in the near term (years to decades).

The region north of Cape Hatteras has been labeled as a "hot spot" where the acceleration of SLR over the past several decades exceeds that of global mean sea level [*Sallenger et al.*, 2012; *Boon*, 2012]. This hot spot of SLR is also prevalent in ocean dynamics models of future regional sea level change [*Yin et al.*, 2009]. It has been attributed to multiple processes including longshore wind forcing [*Piecuch et al.*, 2016], weakening of the Gulf Stream associated with decreased Atlantic Meridional Overturning Circulation (AMOC) [*Ezer et al.*, 2013; *Goddard et al.*, 2015; *Ezer*, 2015], the inverse barometer effect [*Piecuch and Ponte*, 2015], and variability captured in a suite of ocean-atmosphere indices [*Kopp*, 2013]. Empirical evidence for a connection between the AMOC and the sea level hot spot comes from an abrupt SLR in 2009–2010 north of Cape Hatteras that occurred in concert with a 30% reduction in the AMOC [*Goddard et al.*, 2015], in addition to an observed AMOC decline from 2004 to 2014 [*Srokosz and Bryden*, 2015]. The mechanistic link between AMOC strength and coastal sea level north of Cape Hatteras is thought to be related to the mass redistribution of water onto the North American shelf produced by changes in strength (and heat transfer) of the western boundary current [*Ezer et al.*, 2013; *Goddard et al.*, 2015; *Ezer*, 2015]. Nonetheless, the causal link between AMOC intensity and the sea level hot spot on decadal scales remains debated, in part due to the short length of the observational period [*Kopp*, 2013]. Additionally, despite temporal correspondence to AMOC weakening and longshore wind forcing [*Piecuch et al.*, 2016], the inverse barometer effect may explain up to 50% of the SLR signal for the 2009–202010 event and ~10–30% of the multidecadal sea level signal [*Piecuch and Ponte*, 2015]. Recent work demonstrates that AMOC weakening must exceed a threshold to have an effect on sea level north of Cape Hatteras; hence, it may be difficult to discern a clear relation between coastal sea level and AMOC strength over the past decades [*Little et al.*, 2017]. The sea level gradient between the

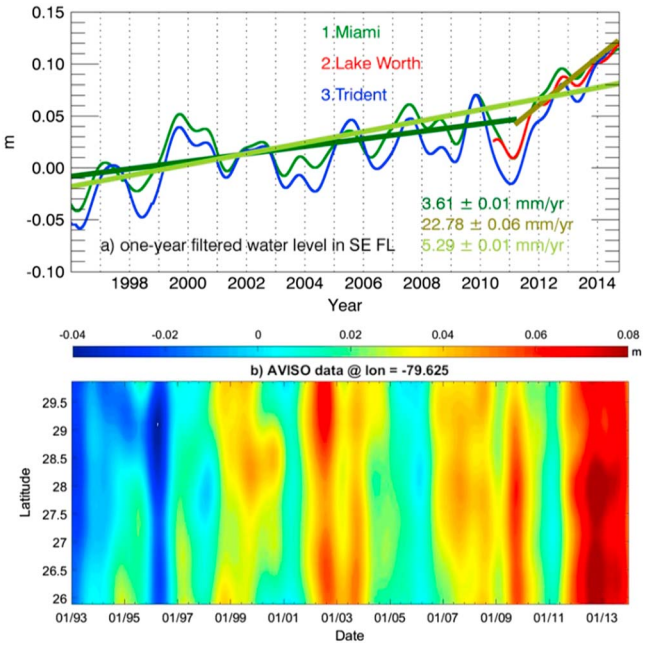

Figure 1. (a) One-year filtered sea level position at three stations in Southeastern Florida. These data show the relatively persistent increase in sea level in Florida at three stations after 2010. The SLR rates shown on the figure are for the station in Miami. (b) Hovmöller diagram of one-year filtered sea level (m) off Florida's coast from AVISO. This illustrates the increased water level after 2010 that is seen in the tide gauge records shown in Figure 1a. The rates of SLR averaged over all latitudes of this transect are 2.3 ± 0.4 mm/yr for the period of 1993–2010, 15.8 ± 2.3 mm/yr after 2010, and 2.8 ± 0.2 mm/yr for the entire period (1993–2014).

regions north and south of Cape Hatteras seems to correlate with multidecadal-scale variations in ocean-atmosphere dynamics including the Atlantic Multidecadal Oscillation (AMO) [*McCarthy et al.*, 2015], Gulf Stream North Wall index [*Taylor and Stephens*, 1998], and the North Atlantic Oscillation (NAO) [*Kopp*, 2013; *McCarthy et al.*, 2015]. Taken together, these studies suggest multiple potential driving mechanisms for sea level change along the eastern U.S. that superimpose in space and time.

Here we investigate a recent, pronounced acceleration in SLR from 2011 to 2015 that is focused south of Cape Hatteras [*Park and Sweet*, 2015; *Wdowinski et al.*, 2016], where variability in AMOC strength should not have a pronounced effect on coastal sea level [*Bingham and Hughes*, 2009]. This acceleration requires a different explanation than AMOC weakening because (1) simultaneous AMOC measurements indicate no significant change from 2011 to 2014 [*Srokosz and Bryden*, 2015] and (2) the acceleration in the south is associated with a deceleration in SLR north of the Cape, the region where enhanced SLR is expected during AMOC weakening.

2. Methods

To explore the mechanism driving recent changes in sea level, we analyzed salient spatiotemporal patterns of SLR along the eastern U.S. over the last 95 years (1920–2015). Sea level data were compiled for the east coast of the U.S. from Florida to Maine (Figure S1 in the supporting information) from two sea level data repositories: Hawaii Sea Level Center (uhslc.soest.hawaii.edu) and NOAA's tide stations (tidesandcurrents.noaa.gov). The Hawaii Sea Level Center provided hourly data from 1 January 1920 to 31 December 2012 ("long period") at stations in white letters. NOAA provided data from 1 January 1996 to 1 May 2015 ("short period") at stations in red numbers. The short period represents the last 19 years, or one full nodal tidal cycle, following the convention adopted by the National Ocean Service to represent the time segment over which tide observations are taken to obtain mean values. The short period also spanned a shorter distance, from Florida to New York, relative to the long period, which extended to the Canada-United States border. A few stations report data beginning at later dates than those mentioned above. The inverse barometer effect was not removed from the data shown because its removal does not alter the essence of the results. In addition, wind mean speeds and gust speeds were compiled from 1987 to 2015 from the National Data Buoy Center stations at NOAA buoys 41009, 41008, 41004, 41037, 41025, CHLV2, 44009, 44065, and 44018 from off Mayport, Florida, to off Cape Cod. The chosen stations are approximately 20 nautical miles east of coast. Data were compiled to analyze other atmospheric forcings that could produce sea level change.

In order to identify recent changes in sea level rise, sea level data from all stations, and for both the long and short periods, were detrended (linear trend) and filtered with a cosine Lanczos filter [*Thomson and Emery*, 2014] centered at 365 days. This filter smoothed out monthly, seasonal, and semiannual variations in sea level

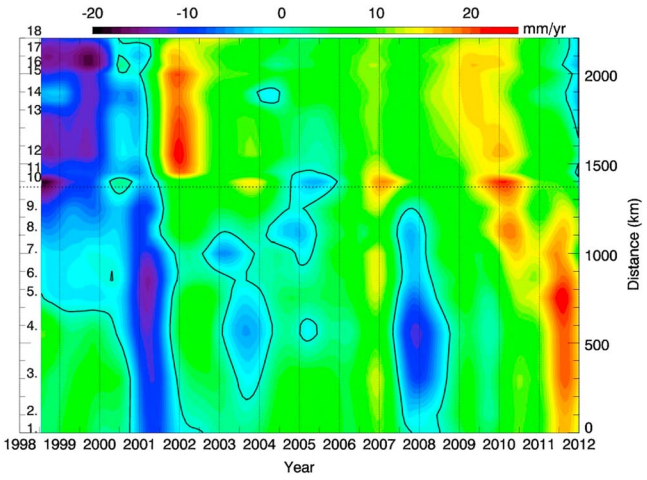

Figure 2. Hovmöller or phase diagram for the 5 year rates of sea level change (in mm/yr) related to the short period time series. The horizontal dotted line represents the location of Cape Hatteras. The black contours represent zero values. The numbers on the ordinate correspond to locations on Figure S1. The tick labels on the horizontal axis appear in the middle of each year.

(e.g., Figure 1a for the short period at three stations in south Florida). One-year low-pass filtering resulted in loss of one half year at the beginning and end of the time series.

One-year low-pass-filtered data of water level were arranged in Hovmöller (or phase) diagrams for most of the eastern seaboard of the United States at uniformly gridded values at intervals of 30 days and 50 km. Phase diagrams display the propagation of signals in space and time, in this case of sea level increase or decrease. These diagrams were constructed with the long and the short periods to identify spatial structures and magnitudes of the interannual variability. One-year filtered hourly data from recording stations were interpolated to this uniform space-time grid with Delaunay triangulations [*Fang and Piegl*, 1992, 1993]. This technique provides optimal interpolations by constructing triangles with vertices at each data point. In addition, all circumcircles associated with each triangle have no data points in their interior.

One-year filtered time series over the long period, as portrayed in the phase diagram, were then decomposed into empirical orthogonal functions (EOFs). The EOF analysis was performed only on the long-period phase diagrams to ensure statistical reliability. These functions depict the spatial structure of sea level variability throughout the eastern United States and the temporal variations, from 1921 to 2011, of those spatial structures. Interpolating between the tide gauge stations does not affect our interpretation.

In addition, linear trends in sea level rise were determined for 5 year periods throughout the span of the long- and short-period observations. Five-year rates were determined from the monthly gridded values of the phase diagram. Similarly, EOF analysis was performed with the 5 year rates of SLR. The two dominant EOF modes obtained with the 5 year rates were compared (via coherence and wavelet coherence analyses) to climate indices, such as El Niño–Southern Oscillation (ENSO), NAO, and AMO but no significant correlation was found (not shown). Finally, cumulative indices were obtained by (1) normalizing (removing the mean and dividing by the standard deviation) the principal components and the climate indices, (2) integrating the normalized variables over time, and (3) smoothing the result of the integration with a 7 year low-pass filter [e.g., *McCarthy et al*., 2015].

3. Results

The short tide gauge records revealed that sea level in southeast Florida, for example, rose at a rate of 3–4 mm/yr from 1996 to 2010 (Figures 1 and 2). This observed rate was between the global mean SLR and ≈33% faster and increased sixfold to >20 mm/yr between 2011 and 2015. A similar acceleration in sea level appeared in all tide gauge records we analyzed south of Cape Hatteras. The observed pattern of sea level change also occurred in the Archiving, Validation, and Interpretation of Satellite Oceanographic (AVISO) altimeter data off the coast of eastern Florida (Figure 1b). Observed patterns prompted our investigation to determine whether such high rates of SLR had previously been recorded in the region south of Cape Hatteras.

The detrended and filtered tide gauge data (Figure S2) were then used to calculate rates of sea level change over consecutive 5 year windows, hereafter referred to as the 5 year rate (Figures 2 and 3). This time window was chosen so that the rates observed from 2011 to 2015 could be directly compared to the rest of the record. The long time series records show the highest positive water level anomalies south of Cape Hatteras in 1947–1948, centered on Cape Hatteras in 1973, and north of Cape Hatteras in 2009–2010 (Figure S2b). These events

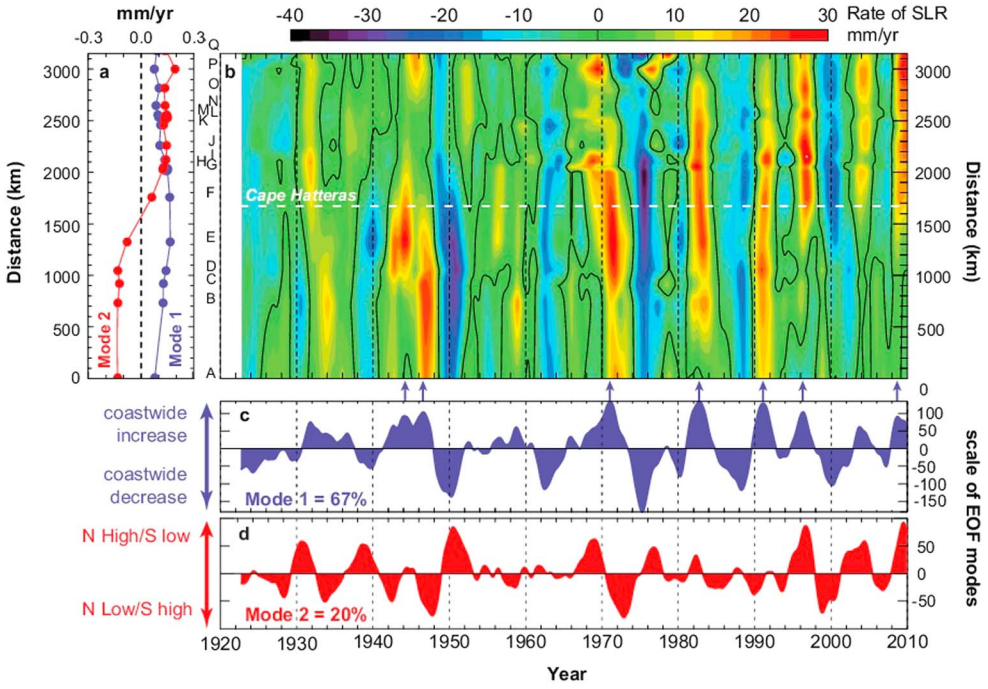

Figure 3. Analysis of the 5 year rates of sea level change (in mm/yr) for the long time series. (a and b) Spatial structure of the first two EOF modes associated with values, which depicts the Hovmöller diagram analogous to Figure 1 (letters relate to Figure S1). (c and d) The scale (or temporal variability) of EOF modes 1 and 2, corresponding to Figure 3a. The blue arrows above Figure 3c show that the highest peaks in Mode 1 correspond to the timing of the SLR hot spots in Figure 3b.

were accompanied by high 5 year rates of SLR (>20 mm/yr) comparable to the rates of SLR recorded south of Cape Hatteras between 2011 and 2015, indicating at least six pulses of SLR (hot spots) on the eastern U.S. (Figure 3). The ephemeral SLR accelerations were typically followed by pronounced decelerations in the rate of SLR, prompting us to hypothesize that the region south of Cape Hatteras is due to experience the same in the near future.

The location of the observed intervals of SLR >20 mm/yr (hereafter referred to as hot spots) migrates over time (Figure 3) and can be observed south of (1947–1948), north of (2009–2010), or approximately centered on (1971–1972) Cape Hatteras, where the Gulf Stream separates from the shelf break. This separation leads to a sea level gradient between the Gulf Stream and cooler, subpolar water from the north. In turn, the gradient has a decisive influence on sea level variations to the north of Cape Hatteras as the strength of the Gulf Stream fluctuates, with only subtle, if any, effects to the south [*Yin et al*., 2009; *Bingham and Hughes*, 2009]. Therefore, the shift of the SLR hot spot from north to south of the Cape from 2009 to 2015 implies a mechanism other than AMOC strength.

To gain further insight regarding the spatial and temporal patterns in sea level variability along this coastline, we performed an empirical orthogonal function (EOF) analysis of the filtered and detrended long time series 5 year rates (Figure 3). The first two EOF modes for the 5 year rates explain 67% and 20% of the variance, respectively, and the spatial patterns of the modes are the same for the sea level position data as for the SLR data that are discussed here (Figure S3). Mode 1 describes coherent rates of sea level rise or fall for the entire eastern U.S. (Figure 3a). Mode 2 describes SLR changes that increase north of Cape Hatteras with a simultaneous drop to the south of the Cape, or vice versa (Figure 3a). The two dominant EOF modes do not directly correlate with climate indices such as the NAO, AMO, or ENSO; nor do they show a direct relationship with wind and wave patterns, atmospheric pressure, or temperature (Figure S4).

Our detection of a coherent rise and fall of sea level observed along the entire coastline (Mode 1; Figure S3) is consistent with previous work [*Yin and Goddard*, 2013; *Woodworth et al*., 2014], but here we also demonstrate a corresponding spatial coherence in the rates of SLR (Mode 1; Figure 3). Coherent changes in sea surface along the U.S. east coast have been attributed to nearshore wind forcing [*Woodworth et al*., 2014] or to net

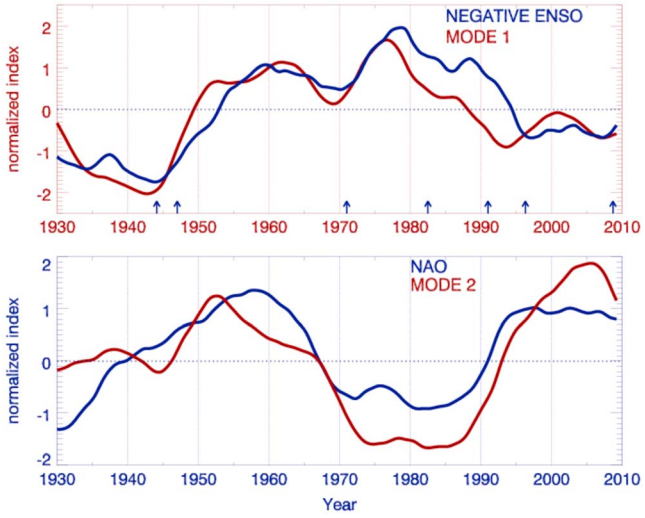

Figure 4. Cumulative and 7 year filtered versions of EOF Mode 1 and negative (top) ENSO index and (bottom) EOF 2 and NAO index. The blue arrows are like those in Figure 3, between Figures 3b and 3c.

vertically integrated zonal transport resulting from meridional variation in the Sverdrup transport over the basin interior [*Thompson and Mitchum*, 2014]. These mechanisms are not necessarily mutually exclusive and could be related to the cumulative effects of wind stress over the North Atlantic. In fact, although we do not find a significant correlation between ENSO and Mode 1 of the EOF (see Figure S3, which shows an inconsistent relationship between the ENSO index and Mode 1), we discovered that the 7 year filtered cumulative index of Mode 1 (coherent change in rate of SLR) of our EOF analysis shows a strong negative correlation with a 7 year filtered cumulative index of ENSO (Figure 4; correlation coefficient of 0.76 and p value of 0.00). This implies that the preexisting state of the subtropical gyre is key to determining the strength of the sea level response rather than a simple correlation between each El Niño/La Niña event and the rate of SLR.

In a conceptual sense, the timing of the SLR hot spots can be attributed to scenarios where the net zonal transport of water into the western boundary region cannot be balanced by meridional divergence through acceleration of the western boundary current and manifests as vertical divergence [*Thompson and Mitchum*, 2014]. We propose that the observed correlation to ENSO derives from the Pacific-North American teleconnection, which is strongest in the winter months. During El Niños, atmospheric pressure at sea level drops in the subequatorial and midlatitude North Atlantic, weakening the northeasterly Trade winds in the Atlantic. This abates the zonal transport of water into the western boundary region while simultaneously amplifying the westerlies and affecting the transport out of the western region of the North Atlantic subtropical gyre [*Xie and Carton*, 2004, and references therein]. Conversely, during La Niña the volume transport increases into the western portion but the outflowing volume transport decreases. This explains the observed anticorrelation between the cumulative ENSO index and the coherent sea level rise along the eastern U.S. captured in the cumulative Mode 1 of the EOF analysis (Figure 4). This volume transport mechanism is supported by modeling studies that show that meridional variations in the wind-stress-curl [*Hong et al*., 2000] and in the zonal volume transport [*Thompson and Mitchum*, 2014] are essential to account for sea level variability in the western boundary region.

While the net zonal transport of water into and out of the western boundary region is related to the timing of the SLR hot spots, their latitudinal position is variable. The north-south sea level gradient that emerges in Mode 2 of the EOF analysis reflects a pattern of regional sea level variability shown elsewhere [*Kopp*, 2013; *McCarthy et al*., 2015]. This pattern results from changes in the strength of ocean circulation that are driven by the NAO through changes in buoyancy forcing and wind-driven ocean circulation [*Marshall et al*., 2001; *McCarthy et al*., 2015]. We confirm that the cumulative index of Mode 2 correlates with a cumulative index of the NAO with a 1 to 2 year lag (correlation coefficient of 0.68 and p value of 0.00) related to the upstream ocean circulation driven by wind. This correlation is similar to the findings of *McCarthy et al*. [2015], who analyzed sea level position, but here we have demonstrated that this pattern also holds for the rates of SLR (Figure 4). The cumulative indices of Modes 1 and 2 represent the inertia (or memory) kept by the ocean from the influence of these intradecadal ocean-atmosphere oscillations. In this sense, the NAO forcing of Mode 2 serves to focus the SLR signal latitudinally, and the SLR hot spots themselves manifest at times when the net zonal transport of water into the western boundary region cannot be accommodated through meridional divergence.

The decline of the AMOC has previously gained the most traction as an explanation for the past acceleration of SLR north of Cape Hatteras, in part, because it is a consistent feature in ocean dynamic modeling of the evolution of regional sea level change patterns in the context of global warming [*Yin et al*., 2009; *Bingham and Hughes*, 2009]. While this effect may come to bear as the result of a weakening AMOC, the argument cannot explain the recent shift in the rates of regional SLR that we have documented south of Cape Hatteras. The AMOC did not weaken from 2011 to 2014 (data for 2015 not yet available) [*Srokosz and Bryden*, 2015; *Church et al*., 2013; *Rahmstorf et al*., 2015] and there is no mechanism to link AMOC strength with such a response of sea level south of Cape Hatteras, suggesting that other effects are dominating regional sea level behavior.

4. Conclusions

As global mean sea level continues to climb in the future, extreme events such as storm surges and extreme ("king") tides will be superimposed on a higher base level [*Kemp and Horton*, 2013]. King tides already cause regular incursions of seawater into many coastal communities, where continued SLR is increasing the frequency of this so-called nuisance flooding, which may be further amplified by short-lived SLR hot spots. We have demonstrated that SLR hot spot anomalies are a recurring feature along the U.S. eastern seaboard related to the combined cumulative effects of ENSO and NAO forcing. We conclude that the formerly identified SLR acceleration in the Mid-Atlantic Bight was not primarily driven by a slowing of the AMOC, but that this spatial pattern primarily resulted from the cumulative effects of NAO forcing during periods when SLR was accelerating along the entire eastern seaboard of the U.S. This distinction is critical to the projection of SLR along this heavily populated coastline and defines a new benchmark for ocean dynamic models to capture such a pattern of regional SLR variability. These SLR hot spots are key risk factors for coastal vulnerability in the context of continued global mean SLR that will be critical to capture in models projecting future regional sea level change.

Acknowledgments
We thank M. Olabarrieta, X. Feng, J. Horn, and C. Skidmore for their help with compiling tide and atmospheric data. G. Athie and J. Olascoaga helped us with the AVISO data. This work was supported by OCE-1325227, OCE-1332718, and OCE-1159040. Data for this study were obtained from the Hawaii Sea Level Center (uhslc.soest.hawaii.edu), NOAA's tide stations (tidesandcurrents.noaa.gov), and the Archiving, Validation, and Interpretation of Satellite Oceanographic altimetry data website (AVISO, www.aviso.altimetry.fr/en/my-aviso.html).

References

Bingham, R. J., and C. W. Hughes (2009), Signature of the Atlantic meridional overturning circulation in sea level along the east coast of North America, *Geophys. Res. Lett.*, *36*, L02603, doi:10.1029/2008GL036215.

Boon, J. D. (2012), Evidence of sea level acceleration at US and Canadian tide stations, Atlantic Coast, North America, *J. Coast. Res.*, *28*, 1437–1445.

Church, J. A., et al. (2013), *Climate Change* 2013*: The Physical Science Basis, Contribution of Working Group 1 to the Fifth Assessment Report of the Intergovernmental Panel on Climate Change*, edited by T. F. Stocker et al., Cambridge Univ. Press, Cambridge, U. K.

Ezer, T. (2015), Detecting changes in the transport of the Gulf Stream and the Atlantic overturning circulation from coastal sea level data: The extreme decline in 2009–2010 and estimated variations for 1935–2012, *Global Planet. Change*, *129*, 23–36, doi:10.1016/j.gloplacha.2015.03.002.

Ezer, T., L. P. Atkinson, W. B. Corlett, and J. L. Blanco (2013), Gulf Stream's induced sea level rise and variability along the US mid-Atlantic coast, *J. Geophys. Res. Oceans*, *118*, 685–697, doi:10.1002/jgrc.20091.

Fang, T.-P., and L. A. Piegl (1992), Algorithm for Delaunay triangulation and convex-hull computation using a sparse matrix, *Comput. Aided Des.*, *24*, 425–436.

Fang, T.-P., and L. A. Piegl (1993), Delaunay triangulation using a uniform grid, *IEEE Comput. Graphics Appl.*, *13*, 36–47.

Goddard, P. B., J. Yin, S. M. Griffies, and S. Zhang (2015), An extreme event of sea-level rise along the Northeast coast of North America in 2009–2010, *Nat. Commun.*, *6*, 6346, doi:10.1038/ncomms7346.

Hong, B. G., A. J. Clarke, and W. Sturges (2000), Sea level on the US east coast: Decadal variability caused by open ocean wind-curl forcing, *J. Phys. Oceanogr.*, *30*(8), 2088–2098.

Kemp, A. C., and B. P. Horton (2013), Contribution of relative sea-level rise to historical hurricane flooding in New York City, *J. Quat. Sci.*, *28*, 537–541.

Kopp, R. E. (2013), Does the mid-Atlantic United States sea level acceleration hot spot reflect ocean dynamic variability?, *Geophys. Res. Lett.*, *40*, 3981–3985, doi:10.1002/grl.50781.

Little, C. M., C. G. Piecuch, and R. M. Ponte (2017), On the relationship between the meridional overturning circulation, alongshore wind stress, and United States East Coast sea level in the community Earth system model large ensemble, *J. Geophys. Res. Oceans*, *122*, 4554–4568, doi:10.1002/2017JC012713.

Marshall, J., H. Johnson, and J. Goodman (2001), A study of the interaction of the North Atlantic Oscillation with ocean circulation, *J. Clim.*, *14*, 1399–1421.

McCarthy, G. D., I. D. Haigh, J. J.-M. Hirschi, J. P. Grist, and D. A. Smeed (2015), Ocean impact on decadal Atlantic climate variability revealed by sea-level observations, *Nature*, *521*, 508–510.

Neumann, B., A. T. Vafeidis, J. Zimmermann, and R. J. Nicholls (2015), Future coastal population growth and exposure to sea-level rise and coastal flooding-a global assessment, *PLoS One*, *10*(3), e0118571.

Park, J., and W. Sweet (2015), Accelerated sea level rise and Florida Current transport, *Ocean Sci. Discuss.*, *12*, 551–572.

Piecuch, C. G., and R. M. Ponte (2015), Inverted barometer contributions to recent sea level changes along the northeast coast of North America, *Geophys. Res. Lett.*, *42*, 5918–5925, doi:10.1002/2015GL064580.

Piecuch, C. G., S. Dangendorf, R. M. Ponte, and M. Marcos (2016), Annual sea level changes on the North American Northeast Coast: Influence of local winds and barotropic motions, *J. Clim.*, *29*(13), 4801–4816.

Rahmstorf, S., et al. (2015), Exceptional twentieth-century slowdown in Atlantic Ocean overturning circulation, *Nat. Clim. Change*, *5*, 475–480.

Sallenger, A. H., Jr., K. S. Doran, and P. A. Howd (2012), Hotspot of accelerated sea-level rise on the Atlantic coast of North America, *Nat. Clim. Change*, *2*, 884–888.

Srokosz, M., and H. Bryden (2015), Observing the Atlantic Meridional Overturning Circulation yields a decade of inevitable surprises, *Science*, *348*, 1255575.

Stammer, D., A. Cazenave, R. M. Ponte, and M. E. Tamisiea (2013), Causes for contemporary regional sea level changes, *Annu. Rev. Mar. Sci.*, *5*, 21–46.

Taylor, A. H., and J. A. Stephens (1998), The North Atlantic Oscillation and the latitude of the Gulf Stream, *Tellus A*, *50*(1), 134–142, doi:10.1034/j.1600-0870.1998.00010.x.

Thompson, P. R., and G. T. Mitchum (2014), Coherent sea level variability on the North Atlantic western boundary, *J. Geophys. Res. Oceans*, *119*, 5676–5689, doi:10.1002/2014JC009999.

Thomson, R. E., and W. J. Emery (2014), *Data Analysis Methods in Physical Oceanography*, Elsevier, Waltham, Mass.

Wahl, T., S. Jain, J. Bender, S. D. Meyers, and M. E. Luther (2015), Increasing risk of compound flooding from storm surge and rainfall for major US cities, *Nat. Clim. Change*, *5*, 1093–1097.

Wdowinski, S., R. Bray, B. P. Kirtman, and Z. Wu (2016), Increasing flooding hazard in coastal communities due to rising sea level: Case study of Miami Beach, Florida, *Ocean Coastal Manage.*, *126*, 1–8.

Woodworth, P. L., M. Á. M. Maqueda, V. M. Roussenov, R. G. Williams, and C. W. Hughes (2014), Mean sea-level variability along the northeast American Atlantic coast and the roles of the wind and the overturning circulation, *J. Geophys. Res. Oceans*, *119*, 8916–8935, doi:10.1002/2014JC010520.

Xie, S.-P., and J. A. Carton (2004), Tropical Atlantic variability: Patterns, mechanisms, and impacts, in *Earth Climate: The Ocean-Atmosphere Interaction*, *Geophys. Monogr. Ser.*, edited by C. Wang, S.-P. Xie, and J. A. Carton, pp. 121–142, AGU, Washington, D. C.

Yin, J., and P. B. Goddard (2013), Oceanic control of sea level rise patterns along the East Coast of the United States, *Geophys. Res. Lett.*, *40*, 5514–5520, doi:10.1002/2013GL057992.

Yin, J., M. E. Schlesinger, and R. J. Stouffer (2009), Model projections of rapid sea-level rise on the northeast coast of the United States, *Nat. Geosci.*, *2*, 262–266.